Published by :
https://www.ijert.org/
An International Peer-Reviewed Journal

International Journal of Engineering Research & Technology (IJERT)
ISSN: 2278-0181
Vol. 15 Issue 03 , March - 2026

Numerical Simulation of The Resistance of Tubular Frame Structures in Agricultural Greenhouses

Konan Eric Konan, Aka Stéphane Koffi, Kouadio Michel Kouame,
Technology Laboratory
UFR Sciences of Structures of Matter and Technology
Félix Houphouët-Boigny University, Abidjan, Côte d'Ivoire

***Abstract* - This study is a numerical analysis of the resistance of six main frame geometries of agricultural greenhouse structures. These tubular frame structures are used for high-tech greenhouses of equal span. Gravity is the only external load considered. The different studies were conducted statically using SOLIDWORKS 2023 software. The maximum stresses in the structures are found near the connections between welded components. Horizontal spans experience the greatest deformations. Structures with vertical spans exhibit better strength; the strength of the arched roof structure (factor of safety FOS = 25.21 and maximum resultant displacement U_{max} = 0.59 mm) is greater than that of the triangular roof structure (FOS = 10.59 and U_{max} = 0.78 mm). The resistance of the triangular roof structure with star-shaped spans (FOS = 9.80 and U_{max} = 1.83 mm) is more suitable than that of the arched roof structure with inclined spans (FOS = 10.54 and U_{max} = 4.34 mm) due to its displacement characteristics. The triangular roof structure with inclined spans (FOS = 6.05 and U_{max} = 0.9 mm) and the arched roof structure with star-shaped spans (FOS = 3.01 and U_{max} = 38.89 mm) are unsuitable for agricultural greenhouse use due to their low FOS values. The verticality of the spans and the arched roof shape emerge as key factors in the resistance of greenhouse structures. Even though all the values obtained are relatively similar in a static gravity analysis, our study suggests the robustness of these structures under higher loads.**

Keywords — Simulation, agricultural greenhouse, tubular frame structure, resistance, deformation

I. INTRODUCTION

Agricultural greenhouses appear as an important lever for the development of agricultural activity [1]. This activity occupies a major place in Africa [2]. It is dominant in the Ivorian economy [3]. Several types of greenhouses are observed both in our tropics and elsewhere [4] [5]. Plastic sheet greenhouses have undergone several stages of development and significant improvements. They are very widespread and remain less expensive than glass greenhouses. Moreover, with adherence to certain specifications during their design, they offer significant advantages in terms of functionality [6]. From vertical span structures to star-shaped span structures and inclined structures, we mainly observe arched or triangular roofs. What about the resistance of these different tubular frame greenhouse structures? Our study compares the strength of six greenhouse structure geometries that characterize the aforementioned trends. We focused on the main frame. The geometries are close to standards and what is common; regardless of any reinforcements that may be made, static studies were conducted on each structure using SOLIDWORKS 2023 software [7]. A description of the tools and methodology is provided before discussing the results and various static studies. We will then conclude.

II. TOOLS AND METHODS

A. Greenhouse structure

Fig. 1 shows us some of the greenhouse structures that have been built.

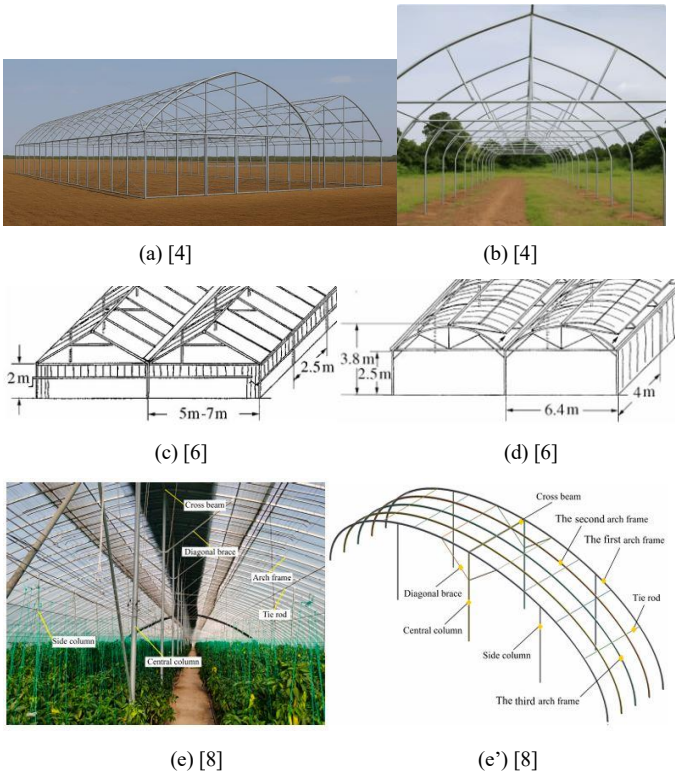

(a) [4] (b) [4]

(c) [6] (d) [6]

(e) [8] (e') [8]

Fig. 1. Greenhouse structures

The structures studied have arched or triangular roofs and their components are made with the same materials. They are generally covered with polyethylene (PE) film [9]. The study addresses the main frames.

The structures consist of monolithic columns, roofs, and spans made of galvanized steel tubing. The spans are either

International Journal of Engineering Research & Technology (IJERT)
ISSN: 2278-0181
Vol. 15 Issue 03 , March - 2026

vertical, inclined at the posts, or star-shaped at 45° on the central post. The materials are the same for each configuration.

The six structural geometries are indicated from A to F in Fig. 2. The inclination of the spans is given relative to the vertical. Except for the five columns and the roof (arched or triangular), the remainder of each structure consists of spans whose 10 m horizontal is supported by the five columns. The welds have a thickness of 27.777 mm.

Column (external diameter 40 mm, thickness 1.5 mm)

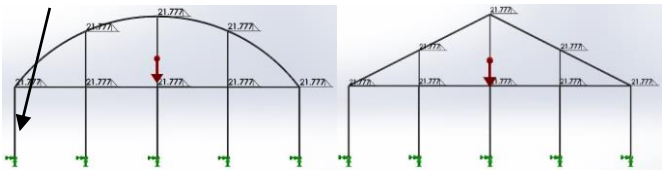

A (vertical span) D

Roof (external diameter 40 mm ep 1.25 mm)

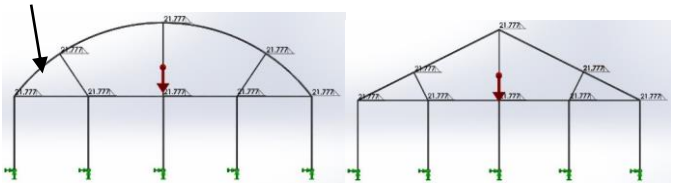

B (inclined at 34°) E (inclined at 27°)

Span (external diameter 25 mm, thickness 1.25 mm)

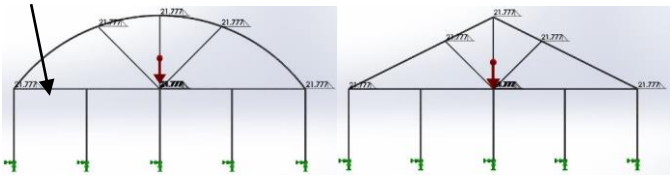

C (45° star-shaped span) F

Fig. 2. Geometry of the structures

Common characteristics of the structures are summarized in Table 1.

TABLE I. COMMON CHARACTERISTICS OF THE STRUCTURES

Parameter designation	Values	Units
Span width	10	m
Ridge height	5	m
Eaves height	2.5	m
Space between columns	2.5	m

B. Modeling

A finite element model of each greenhouse structure was built using SOLIDWORKS 2023 software. Each post is anchored to the ground. All structural components are made of galvanized steel. The constitutive law is Hooke's linear elastic law for isothermal conditions and isotropic bodies:

$$[\varepsilon] = -\frac{\nu}{E}\,\text{trace}\,[\sum]\, I_3 + \frac{1+\nu}{E}[\sum] \qquad (1),$$

with [ε] the strain tensor, ν the Poisson's ratio, E the Young's modulus, I3 the unit matrix and [∑] the stress tensor.

$$[\varepsilon] = \begin{pmatrix} \varepsilon_{11} & \varepsilon_{12} & \varepsilon_{13} \\ \varepsilon_{21} & \varepsilon_{22} & \varepsilon_{23} \\ \varepsilon_{31} & \varepsilon_{32} & \varepsilon_{33} \end{pmatrix} \quad (2) \qquad [\sum] = \begin{pmatrix} \sigma_{11} & \sigma_{12} & \sigma_{13} \\ \sigma_{21} & \sigma_{22} & \sigma_{23} \\ \sigma_{31} & \sigma_{32} & \sigma_{33} \end{pmatrix} \quad (3)$$

The expression for unit strain in the first direction, for example, is:

$$\varepsilon_{11} = \frac{1}{E}[\,\sigma_{11} - \nu\,(\sigma_{22} + \sigma_{33})] = \frac{\Delta l_1}{l_1} \qquad (4),$$

with Δl_1: the elongation and l_1: the initial length.

The equivalent Von Mises stress is determined by:

$$\sigma_{VM} = \sqrt{\sigma^2 + 3\,\tau^2} \qquad (5),$$

with τ: the shear stress, $\tau = \sigma_{ij}$ when i is different from j.

The mechanical properties of the material are shown in Table 2.

TABLE II. PROPRIÉTÉS MÉCANIQUES DE L'ACIER GALVANISÉ

Yield strength σ_e	203.94 MPa
Tensile strength σ_r	356.90 MPa
Elastic modulus **E**	200 GPa
Poisson's ratio **ν**	0.29
Mass density **ρ**	7,870 kg.m^{-3}

The discretization of each structure was performed using average elements. Fig. 3 illustrates the discretization of structure A, for which the minimum and maximum sizes are 8.61 mm and 115.27 mm, respectively.

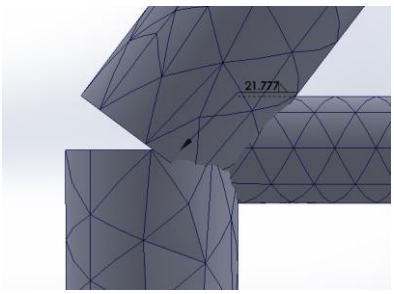

Fig. 3. Discretization

Gravity (g = 9.81 m.s^{-2}) was considered the sole external load. Static studies were conducted.

III. RESULT AND DISCUSUSION

The mass properties of the six structures are practically equivalent (table 3), our analysis addresses three aspects: stresses, deformations and stabilities.

TABLE III. PROPRIÉTÉS MASSIQUES DES STRUCTURES

Structures (roof – spans)	Mass (g)	Volumes (mm^3)	Surfaces areas (mm^2)
A (arc – vertical)	5566.49	5566486.68	8304486.84
B (arc – inclined)	5522.63	5522633.91	8234322.40
C (arc – star-shaped)	5758.58	5758577.45	8611832.08

International Journal of Engineering Research & Technology (IJERT)
ISSN: 2278-0181
Vol. 15 Issue 03 , March - 2026

D (triangular – vertical)	5368.15	5368149.99	7987452.48
E (triangular – inclined)	**5343.53**	**5343534.10**	**7948067.06**
F (triangular – star-shaped)	5574.65	5574645.20	8317844.82
Maximum (C) / Minimum (E) ratio	1.08	1.08	1.08

A. Stress analysis

Fig. 4 shows the distribution of Von Mises stress in the different structures. The deformation scale is 200 for better visibility of the most deformed components.

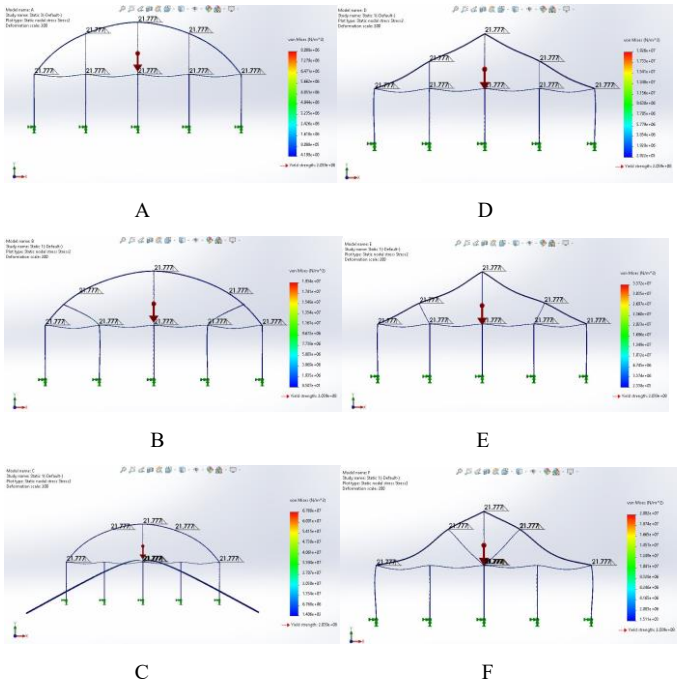

Fig. 4. Von Mises equivalent stress

The maximum Von Mises equivalent stress (σ_{VMmax}) of 8.09 MPa is the lowest for structure A. This implies a factor of safety (FOS) of 25.21. Indeed:

$\sigma_{VMmax} \leq \frac{\sigma_e}{FOS}$ (7), with σ_e = 203.94 MPa : the elastic limit of the material (galvanized steel).

$$\rightarrow \text{FOS} = \frac{\sigma_e}{\sigma_{VMmax}} \quad (8)$$

In order of strength, we have the following structures: D (FOS = 10.59), B (FOS = 10.54), F (FOS = 9.8), E (FOS = 6.05), and C (FOS = 3.01). The factors of safety of structures D, B, and F are similar. They are less than half that of structure A. Those of structures E and C are low compared to the other structures. These last two structures are unsuitable for use as agricultural greenhouses. The maximum Von Mises stress values are observed near the connections between the structural components (Fig. 5). They are largely due to span bending. They are relatively similar across all structures, and the strength of the connections can be reinforced.

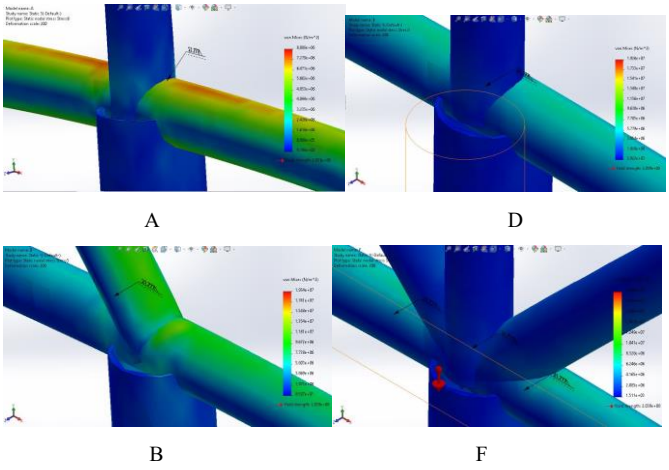

Fig. 5. Distribution of maximum Von Mises stresses

B. Deformation Analysis

Using the same scale of 200 for deformations, Figure 6 shows us the resultant of the displacements of each structure.

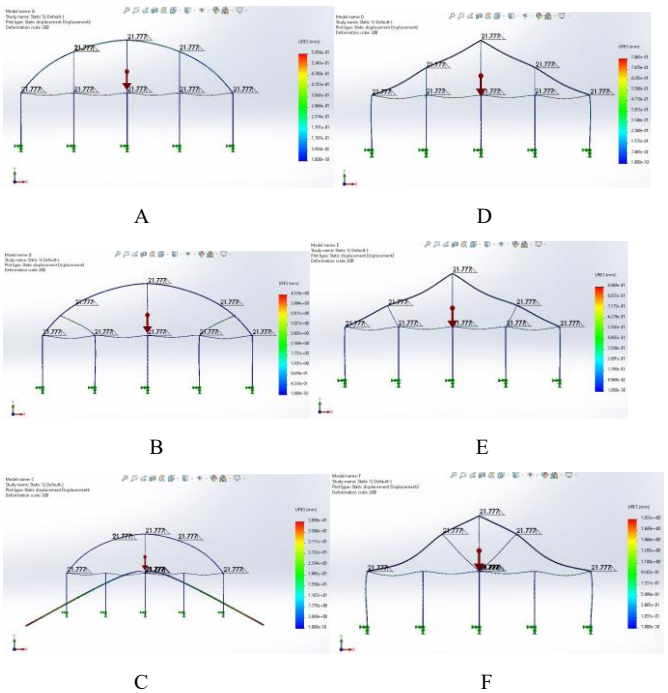

Fig. 6. Resultant displacements

The most significant deformations are observed at the spans. The maximum resultant displacement (U_{max}) of 0.59 mm is lowest for structure A. The same is true for the deformations (ε = 34.78 μ), as shown in Table 4.

International Journal of Engineering Research & Technology (IJERT)
ISSN: 2278-0181
Vol. 15 Issue 03 , March - 2026

TABLE IV. MAIN RESULTS

Structures	Von Mises stress σ_{VMmax} (MPa)	Factor of Safety FOS	Resultant displacements U_{max} (mm)	Equivalent strains ε (μ)
A	**8.09**	**25.21**	**0.59**	**34.78**
B	19.34	10.54	4.34	83.18
C	67.68	3.01	38.89	291
D	19.26	10.59	0.79	82.81
E	33.72	6.05	0.9	145
F	20.82	9.8	1.83	80.56

This suggests better resistance to buckling and other instability phenomena. Next is structure D (U_{max} = 0.79 mm). The subsequent ranking of the lowest maximum resultant displacements is: E (U_{max} = 0.9 mm), F (U_{max} = 1.83 mm), B (U_{max} = 4.34 mm), and C (U_{max} = 38.89 mm). The deformations are not ranked in the same order due to the geometry of the structures: A, F, D, B, E, and C.

The deformation of structure E (ε = 145 μ) is the largest after that of structure C (ε = 291 μ). Structure C is unsuitable. To a lesser extent, structure B is also unsuitable, and attention should be paid to the inclined spans. The inclination of the spans does not appear adequate for arched roofs.

Except for structure A, the rigidity of triangular structures (trusses) is highlighted.

C. Stability Analysis

Based on the main results in Table 3, the arched roof structure with vertical spans A (FOS = 25.21 and U_{max} = 0.59 mm) is more suitable than the other structures. It is followed by the triangular roof structure, also with vertical spans D (FOS = 10.59 and U_{max} = 0.78 mm).

Next, we have the triangular roof structure with star-shaped spans F, compared to the arched roof structure with inclined spans B. Indeed, its resultant displacement is lower (1.83 mm < 4.34 mm) and their factors of safety are similar (9.8 and 10.54, respectively). Slender structures, like ours, are more prone to buckling than compression failure.

The triangular roof structure with inclined spans E and the arched roof structure with star-shaped spans C are unsuitable. Their factors of safety are low (6.05 and 3.01 respectively) and their equivalent deformations are significant (145 and 245 respectively).

The final ranking of the best structures is as follows: A, D, F, B, E, and C.

Two resistance factors emerge, in order of priority, for the best structures (A, D, B, and F):

- 1st: the verticality of the spans (structures A and D),

- 2nd: the arched roof (FOS = 25.21) compared to the triangular roof (10.59)

This is in accordance with Arthur Vierendeel's warning regarding the first factor. He draws attention to the danger of compression members in steel structures. He writes, "It can be said that of ten collapses occurring in steel structures, eight are due to buckling." The eminently dangerous characteristic of compression members is that they fail suddenly without their weakness being revealed to the eye by any obvious sign or warning. Buckling formulas must be used with caution, that is, by taking a very large safety factor. Parts subjected to buckling must be straight and must not have previously undergone deformation [10].

Taking into account the linear buckling analysis using eigenvalues, the Euler stress determined on the central span of length L = 2.5 m, common to all structures, gives us:

$$\sigma_E = P_E/A = \pi^2 EI/(A(kL)^2) = 89.32 \text{ MPa} \quad (9)$$

with: Young's modulus E = 200 GPa, second moment of area $I = 6.5942 \times 10^{-9}$ m⁴, cross-sectional area of column $A = 9.3266 \times 10^{-5}$ m², and support constant (two fixed supports) k = 0.5.

Therefore, we have a safety factor with respect to the critical load due to buckling for this span of:

$$FOS_f = \sigma_e / \sigma_E = 356.9 / 89.32 = 4 \quad (10)$$

This safety margin is sufficient given that the structural load-to-total load ratios are close to this same value [11] for less reinforced structures. Inclined bars, which are more prone to deformation, as mentioned above, require more careful attention when used.

Three inherent instability hazards [12] in any compressed structure can be identified, both locally and globally: buckling, lateral torsional buckling, and web buckling.

Although limited to static studies with gravity as the only external load, our analysis suggests the structural strength for more detailed studies such as double nonlinear buckling analysis [8]. It remains indicative of structural resistance in light of the variability of the various phenomena to be considered (variable loads, non-isothermal environment, etc.).

IV. CONCLUSION

Our study focused on six different greenhouse structures, each representing a specific section of the structure. The static analysis was conducted using SOLIDWORDS 2023 software. The constitutive law applied was Hooke's law for isothermal environments and isotropic bodies. The materials used for the components (columns, roofs, and spans) of the six structures were common. The geometries of the structures differed.

Two resistance factors emerged, in order of priority:

- 1st: the verticality of the spans (structures A and D),

- 2nd: the arched roof (FOS 25.21) compared to the triangular roof (FOS 10.59).

The spans experienced the greatest deformations. Those that were inclined were more prone to deformation. The maximum stresses were located near the connections, which could be reinforced.

Our analysis, beyond these limits, provides an indication of the greenhouse structure's resistance.

International Journal of Engineering Research & Technology (IJERT)
ISSN: 2278-0181
Vol. 15 Issue 03 , March - 2026

REFERENCES

[1] Larouche-Tremblay, M., Ouellet-Plamondon, C. & Godbout, S. (2025). Transfert des connaissances tacites et explicites de l'agriculture traditionnelle vers l'agriculture moderne contrôlée : le cas d'un exploitant de serres verticales dans un environnement nordique. Revue Organisations & territoires, 34(1), 184–208. https://doi.org/10.1522/revueot.v34n1.1920

[2] Pierre Jacquemot. De l'insécurité à la souveraineté alimentaire en Afrique. Willagri-UM6P. 2023. (hal-04314189)

[3] OUGUEHI , K.P. et BAMBA, Y. 2025. Pour une croissance économique durable en Côte d'Ivoire, entre l'agriculture d'exportation et l'agriculture de subsistance, quel type d'agriculture à privilégier ? Une analyse économétrique à travers le modèle ARDL. *Revue Française d'Economie et de Gestion*. 6, 8 (août 2025).

[4] https://serreivoire.pro, accessed on 02 March 2026

[5] Fernández-García, M.S.; Vidal-López, P.; Rodríguez-Robles, D.; Villar-García, J.R.; Agujetas, R. Numerical Simulation of Multi-Span Greenhouse Structures. *Agriculture* 2020, *10*, 499. https://doi.org/10.3390/agriculture10110499

[6] B. von Elsner, D. Briassoulis, D. Waaijenberg, A. Mistriotis, Chr. von Zabeltitz, J. Gratraud, G. Russo, R. Suay-Cortes, Review of Structural and Functional Characteristics of Greenhouses in European Union Countries, Part II: Typical Designs, Journal of Agricultural Engineering Research, Volume 75, Issue 2, 2000, Pages 111-126, ISSN 0021-8634, https://doi.org/10.1006/jaer.1999.0512.

[7] SOLIDWORKS is a software developed by Dassault Systèmes

[8] Dong, X.; Piao, F.; Du, N.; Dong, H.; Zhang, T.; Qin, Y.; Li, Y.; Guo, Z. Optimization of Structural Configuration and Ridge Height for Large-Span Insulated Plastic Greenhouse Based on Finite Element Analysis. *Agriculture* **2025**, *15*, 1333. https://doi.org/10.3390/agriculture15131333

[9] Sagar Maitra, Dinkar J Gaikwad and Tanmoy Shankar, Green-houses: Types and Structural Components. In : Protected Cultivation and Smart Agriculture, © New Delhi Publishers, New Delhi : (2020), (pp. 09-17). ISBN: 978-81-948993-2-7, DOI: 10.30954/NDP-PCSA.2020.2

[10] Radelet-de Grave, P. (2024). Arthur Vierendeel: The Man with Iron Nerves Who Invented the Truss Without Diagonals. In: Between Mechanics and Architecture. Mathematics and the Built Environment, vol 8. Birkhäuser, Cham. https://doi.org/10.1007/978-3-031-73530-1_19

[11] Nefise Yasemin Emekli, Berna Kendirli and Ahmet Kurunc. "Structural analysis and functional characteristics of greenhouses in the Mediterranean region of Turkey." African Journal of Biotechnology 9, no. 21 (2010): 3131-3139. https://doi.org/10.5897/AJB2010.000-3154

[12] Dieudonné Bazonga , Étude expérimentale du comportement en flambement local des pylônes tubulaires (2010), Université de Sherbrooke, https://hdl.handle.net/11143/1518